



Study on Controlling Parameters and Technological Optimization of Strip Longwall Top Coal Caving in Thick Coal Seams

Bui MANH TUNG^{1,*}, Le TIEN DUNG¹, Liu CHANG YOU², Pham VAN CHUNG³

¹) Department of Underground Mining, Hanoi University of Mining and Geology, Hanoi, Vietnam; email: buimanhtung@humg.edu.vn; t.d.le@humg.edu.vn

²) School of mines China University of Mining and Technology, Xuzhou City, China; email:

³) Department of Mine Surveying, Hanoi University of Mining and Geology, Hanoi, Vietnam; email: phamvanchung@humg.edu.vn

<http://doi.org/10.29227/IM-2020-02-14>

Submission date: 06-03-2020 | Review date: 22-09-2020

Abstract

Based on the geological and mining conditions of face 3107 at Liang Baoshi coal mine, China, the numerical programs FLAC3D 2.10 and PFC2D 2.10 were used to analyze the parameters controlling the failure, caving and the coal recovery rate in Strip Longwall Top Coal Caving (SLTCC). The analyzed parameters are face length in dip direction, mining height, the span of coal caving, and sequence of coal drawing. The results show that the application of SLTCC for a limited face length is not favourable to coal failure, and it increases top coal loss. A sound engineering selection of technological parameters is therefore important to efficient mining in thick coal seams. The numerical results show that a face design of 3 m of cutting height, 0.8 m of caving span, and alternate drawing sequence results in high coal recovery rate, simple mining tasks, and efficient operation of face equipment.

Keywords: strip fully-mechanized caving, work face, caving technology, coal recovery rate

1. Introduction

Fully mechanized longwall top coal caving is one of the technologies applying for extraction of thick coal seams in developed coal industries in the world. One limitation of this technology raised from practice is that coal loss during top coal caving process remains large [BUI, M.T, 2014]. Particularly, in cases where the geological condition is unfavourable, the coal seam is spontaneous combustion or panel with large dimension in dip direction is not applicable, Strip Longwall Top Coal Caving (SLTCC) can be installed, but it causes failure, caving and the top coal recovery rate are significantly impacted. Many studies from Vietnam and in the world have used theoretical, physical and numerical modelling methods to analyze the effect of technological parameters on failure and caving mechanics as well as top coal recovery ability [CAO.S.G, 2001., LE,T.D 2018]. These studies, however, are mostly for conventional longwall rather than strip longwall.

This study was carried out at face 3107 of Liang Baoshi coal mine, China. The coal seam is prone to spontaneous combustion with the time of storing temperature from three to six months; the shortest time is 22 days. The applied technology is SLTCC with 81 m length in dip direction. The continuum-based numerical program FLAC3D 2.10 was used to study the failure progress in top coal, while the discontinuum-based numerical program PFC2D 2.10 was employed to investigate the drawing law of top coal and coal recovery rates in a parametric study. The controlling parameters such as face length in dip direction, cutting height, caving span and sequence of drawing are optimized, which should increase the productivity and efficiency in SLTCC operation.

2. Geological condition of the mine site

The fully mechanized SLTCC face 3107 of Seam #3, Liang Baoshi coal mine, FeiCheng Mineral Corporation, Shan Dong, China has a seam thickness of 7.14–9.0 m with an average of 7.9 m. The seam dip is 6–13 degrees with an average of 9 degrees. The face length in dip direction is 81 m, and that in strike direction is 2015 m. The cutting height and caving height are 3 and 5 m, respectively. The thickness of immediate roof is 1.5–5.5 m. The thickness of main roof is 9–33 m and is 25.5 m on average. The overburden depth is 700 m. The mechanical properties of coal and rock are shown in Table 1. Stratigraphic sequence, lithology and depth are displayed in Figure 1.

3. Effect of key parameter on coal caving ability

3.1 Model development

Based on the geological condition of face 3107, FLAC3D 2.10 was used to study the impact of face length (in dip direction) and cutting height on failure and caving of top coal and roof rock at face. The thicknesses of the seam and surrounding strata in the model were similar to those in practice. Since the dip angle of the seam was small, the seam was modelled horizontally. The four side boundaries and bottom boundary were assigned with displacement boundary. That is, the displacement in normal direction was fixed at zero. The top boundary was assigned with stress boundary condition. The model size was 300 m in strike direction, 300 m in dip direction, and 150 m in the vertical direction with equivalent stress for overburden applied on the top boundary. The equivalent stress was calculated as follows:

$$p = \sum H \rho g$$

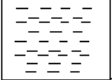
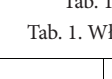
| Columnar | Rock name | Depth (m) | Lithology |
|---|----------------|-----------|---|
|  | Fine sandstone | 21.5 | Light gray to dark gray, fine sand-like structure, interbedded with claystone |
|  | Siltstone | 25.5 | Dark gray to dark gray, silt-like structure, locally with carbide surface |
|  | Carbargilite | 0.8 | Black, massive, muddy structure of carbon-containing fossil plant roots |
|  | Gnt-sandstone | 5.5 | Light gray, coarse sand-like structure, with a fracture |
|  | 3# coal | 7.9 | Black, shiny glass |
|  | Claystone | 21.5 | Black to dark gray, muddy structure, calcite and pyrite-containing films |

Fig. 1. Generalized geological section
Rys. 1. Uogólniony przekrój geologiczny

Tab. 1. Mechanical of coal and rock properties
Tab. 1. Właściwości fizyczno-mechaniczne węgla i skał

| Name | | Density | Young modulus | Poisson ratio | Cohesion | Internal friction angle | Tensile strength |
|------------|----------------|-----------------------|------------------------|---------------|----------|-------------------------|----------------------|
| | | D(kg/m ³) | E (MPa) | m | c (MPa) | φ(°) | σ _t (MPa) |
| Roof rock | Siltstone | 2460 | 1.95x10 ⁴ | 0.2 | 2.75 | 38 | 1.84 |
| | Mudstone | 2461 | 0.875x10 ⁴ | 0.26 | 1.2 | 30 | 0.605 |
| | Sandy mudstone | 2510 | 0.5425x10 ⁴ | 0.147 | 2.16 | 36 | 0.75 |
| | Fine sandstone | 2873 | 3.34x10 ⁴ | 0.235 | 3.2 | 42 | 1.29 |
| | sandstone | 2487 | 1.35x10 ⁴ | 0.123 | 2.06 | 40 | 1.13 |
| Coal seam | Coal | 1380 | 0.53x10 ⁴ | 0.32 | 1.25 | 32 | 0.15 |
| | Mudstone | 2483 | 1.77x10 ⁴ | 0.204 | 1.2 | 32 | 0.58 |
| Floor rock | Fine sandstone | 2460 | 1.95x10 ⁴ | 0.2 | 3.75 | 38 | 1.84 |
| | Siltstone | 2580 | 2.5x10 ⁴ | 0.159 | 2.5 | 42 | 3.6 |
| | Sandy mudstone | 2530 | 1.085x10 ⁴ | 0.147 | 2.45 | 40 | 2.01 |

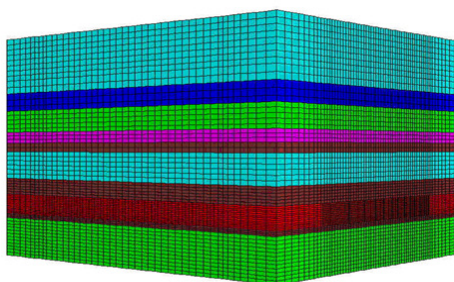


Fig. 2. Numerical Simulation Model by FLAC3D 2.10
Rys. 2. Symulacyjny numeryczny model według FLAC3D 2.10

Where H – is the thickness of overburden, m ; g is gravity = 9.81 m/s². The model extracts a seam thickness of 7.9 m, and has a total of 45333 zones and 53490 grid-points. The mechanical properties of coal and rock are taken from Table 1.

To study the effect of face length on caving behavior, different values of 60, 80, 100, 120, 150 and 180 m were modelled. Similarly, different cutting heights of 2.0, 2.4, 2.8, 3.2, 3.6 and 4.0 m were modelled to study the effect of cutting height on model behaviour.

3.2 Effect of face length (in dip direction)

The caving state of top coal when face length varies is displayed in Figure 3. It is seen that different face lengths resulted in different states of top coal caving. However, when the face length exceeded a certain value, the state did not change significantly.

When the face length was 60 m, the caving state was not very ideal, especially at two gate ends. The roof seriously hanged and caved in massive that caused low rate of top coal recovery. When the length reached 80 m, caving state was improved. However, the caving still occurred mainly in the mid-

dle of the length. At the two gate ends, due to protective pillar or coal face, the roof hanging and caving delay still occurred. The coal loss here would be high if there was no technical solution. When the face length increased to 100, 120, 150 and 180 m, the state was clearly improved. Beyond 150 m, the state was ideal. This result is in agreement with practical experience that as the face length increases, the top coal loss at gate ends decreases.

Change in face length led to change in caving height of top coal. When the length increased from 60 to 80 m, the caving height extended from 4 to 8 m. The caving height increased as the face length increased. When the length reached beyond 150 m, the caving height did not increase remarkably; it stabilized at approximately 37 m. The relationship between face length and top coal caving height is outlined in Figure 4.

3.3 Effect of cutting height

In this sub-section, the face was modelled with a cutting height of 2.0, 2.4, 2.8, 3.2, 3.6 and 4.0 m. The face length was kept unchanged of 80 m. Figure 5 displays the top coal failure state when cutting height varies.

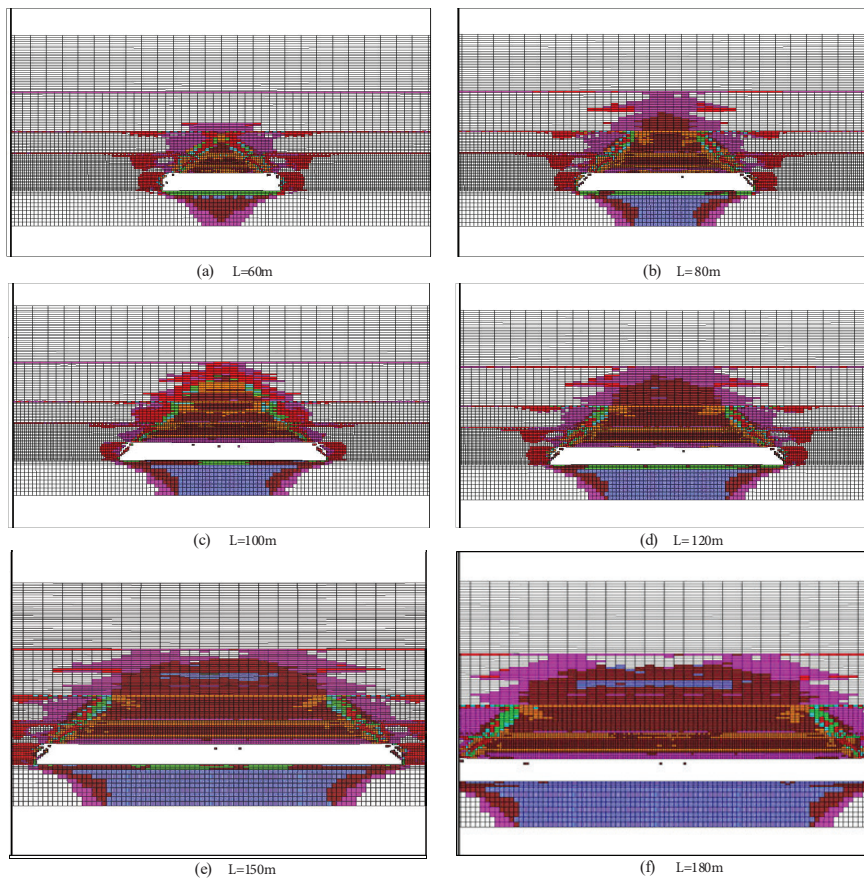


Fig. 3. Top coal caving states in different face lengths
 Rys. 3. Stropowe stany zawałowe przy różnych długościach ścian

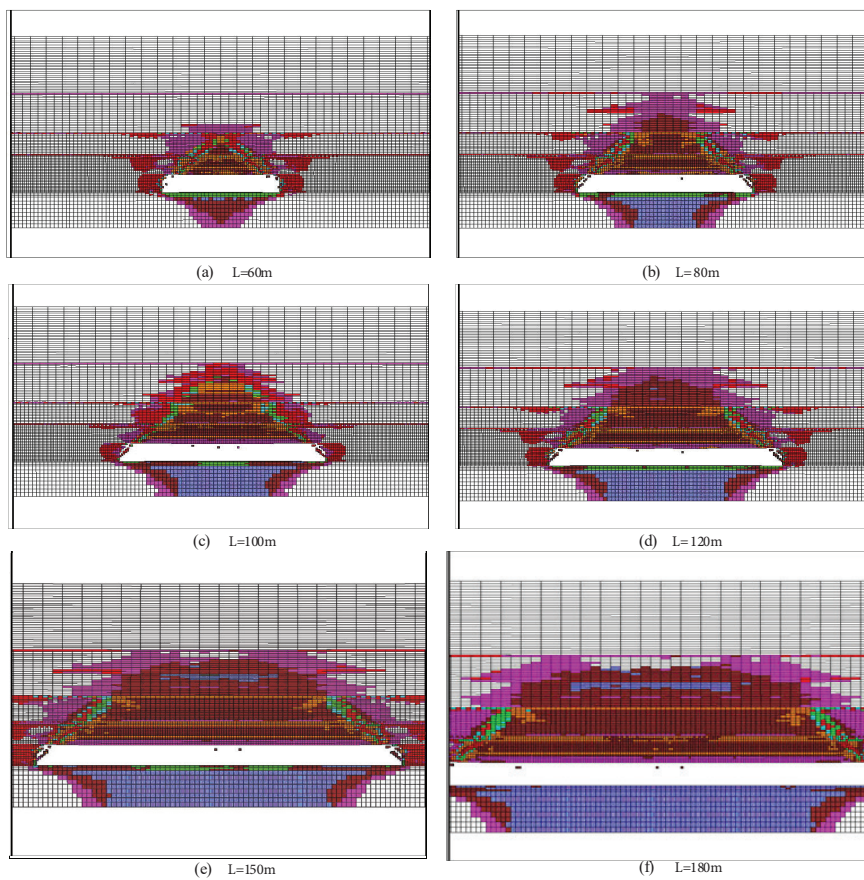


Fig. 3. Top coal caving states in different face lengths
 Rys. 3. Stropowe stany zawałowe przy różnych długościach ścian

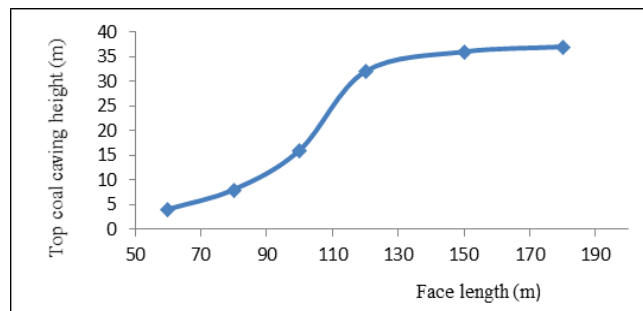


Fig. 4. Relationship between face length and height of top coal caving
Rys. 4. Zależność między długością ściany a wysokością zawалу węgla

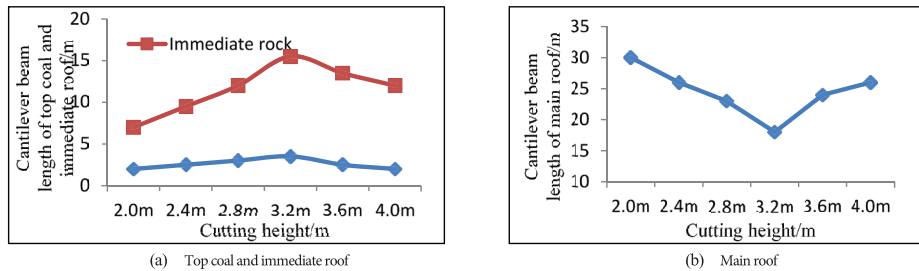


Fig. 6. Relationship between cutting height and cantilever beam length
Rys. 6. Zależność między wysokością urabiania a długością belki wspornikowej

Tab. 2. Physical properties of various rock layers in the model

Tab. 2. Właściwości fizyczne różnych warstw skał w modelu

| Layer | Normal stiffness/Gpa | Shear stiffness/Gpa | Density/kg/m ³ | Particle radius/m | Porosity ratio | Friction coefficient |
|----------------|----------------------|---------------------|---------------------------|-------------------|----------------|----------------------|
| Lower coal | 4 | 4 | 1380 | 0.12 | 0.35 | 0.5 |
| Upper coal | 4 | 4 | 1380 | 0.13 | 0.35 | 0.5 |
| Immediate roof | 4 | 4 | 2550 | 0.15 | 0.35 | 0.5 |

Tab. 3. Calculation result of top coal recovery rate in different caving spans

Tab. 3. Wynik obliczenia najwyższej szybkości odzysku węgla w różnych przedziałach zawalowych

| | | |
|-----------------------------------|-------|-------|
| Caving span/m | 0.8 m | 1.6 m |
| Absolute top coal recovery rate % | 63.76 | 60.54 |
| Relative top coal recovery rate % | 87.04 | 81.98 |

Figure 4 indicates that in different cutting heights, the level of roof caving was also different and top coal caved in separate layers. In an interval of 2–5 m above the cutting coal section, top coal, immediate roof and the main roof formed cantilever beams. The beams had different lengths that ruptured with a delay in the order of from high to low beam. This was the main reason for the top coal loss. The relationship between cutting height and cantilever beam length is provided in Figure 6. The shear zone was distributed about 4–6 m ahead of face line, and there was no tensile failure.

The graph in Figure 6 reveals that when the cutting height was in a range of 2.0–3.2 m, the cantilever beam length of top coal varied in a range of 2–4 m. The length of the immediate roof beam was proportional to cutting height, which increased accordingly from 5 to 12 m. The length of the main roof beam, however, was inversely proportional to cutting height, which decreased from 30 to 18 m. When the cutting height exceeded 3.2 m, the length of top coal and immediate roof beams tended to decrease slightly, from 4 to 2 m and 12 to 10 m, respectively. At the same time, the length of the main roof beam tended to increase from 18 to 26 m. It is seen

that as the cutting height increased, the failure and caving of top coal became easier. However, when the height was larger than 3.2 m, the roofs became less stable. The face spall and top coal fall occurred that interrupt normal production. It can be concluded that for the geological condition of face 3107, a designed cutting height of 3.0 m should maximize top coal recovery rate.

4. Optimization of Technological Parameters

4.1 Model development

Based on the geological condition of face 3107, Liang Baoshi coal mine, the numerical program PFC2D 2.10 was used to optimize the technological parameters of SLTCC. The parameters here are caving span and drawing sequence of top coal.

The model was designed with a length of 22 m, a height of 10.9 m, a cutting height of 2.8 m, a top coal thickness of 5.1 m, and an immediate roof thickness of 3.0 m. On-site observation points out that top coal was divided into upper and lower layers. Top coal layer radii after failure were 0.12 and 0.13 m, respectively. For simulation, immediate roof thickness was similar to that in practice, while the top coal radius was

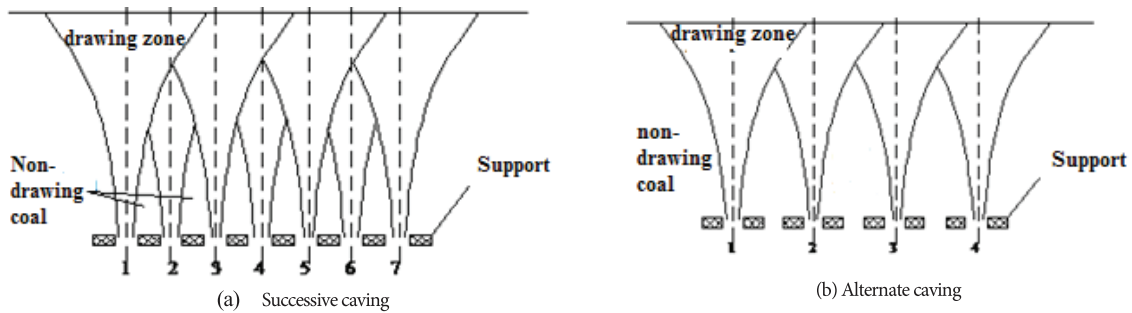


Fig. 7. Caving sequence for top coal
Rys. 7. Kolejność zawału stropowego węgla

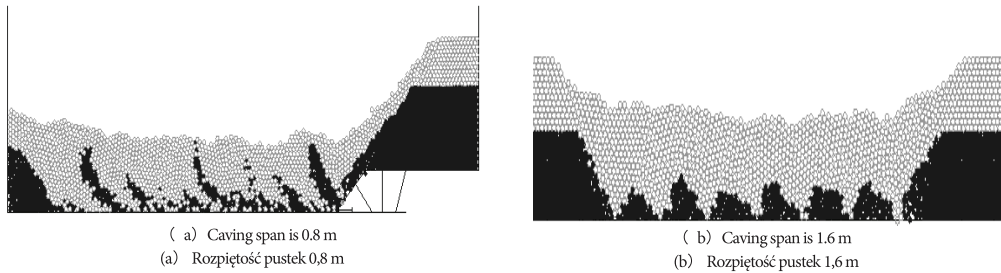


Fig. 8. Top coal loss under different caving spans
Rys. 8. Strata stropowego węgla przy różnych rozpiętościach zawałów



Fig. 9. Distribution of interface between coal and waste rock in successive caving sequence
Rys. 9. Rozkład węgla i stropowej skały w kolejnej sekwencji zawału

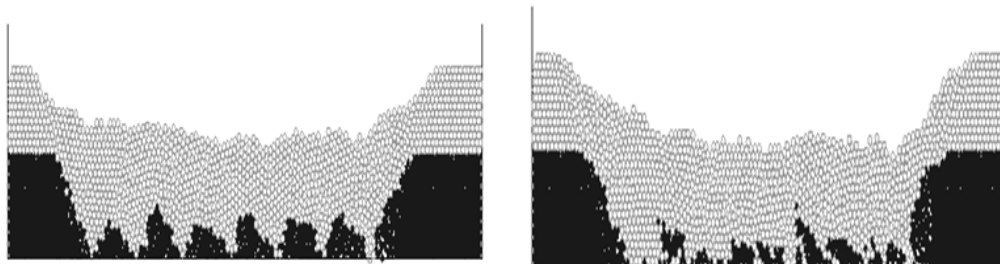


Fig. 10. Interface between coal and waste rock in odd number supports in the alternate drawing sequence
Fig. 11. Interface between coal and waste rock in even number supports in the alternate drawing sequence

assigned to 0.15 m. Physical properties of various rock layers are summarized in Table 2.

For studying the span of top coal caving, two-span lengths of 0.8 and 1.6 m were modelled with the same cutting-caving height ratio of 1:2. The principle for drawing coal is that the recovery process ends when waste rock occurs. The post-processing parameters are caving state, absolute recovery rate and relative recovery rate of top coal.

For studying drawing sequence, a caving span of 0.8 m and cutting-caving height ratio of 1:2 were used. Two sequences, namely successive drawing and alternate drawing,

were investigated (Figure 7). The distribution law of interface between top coal and roof rock and the top coal recovery rate was determined.

4.2 Optimization of caving span

Absolute top coal recovery rate is defined as the ratio of top coal weight recovered in one caving cycle to total coal weight in model. Relative top coal recovery rate is defined as the ratio of top coal weight recovered in one cycle to total coal weight in total face advances. The proposal of the two definitions aims to remove any errors in calculation caused by pre-

Tab. 4. Recovery rate in two drawing sequences
 Tab. 4. Wskaźnik odzysku stropowego węgla z dwóch kolejności zawałowania

| | Top coal recovery rate % | Coal seam recovery rate /% |
|-----------------------------|--------------------------|----------------------------|
| Successive drawing sequence | 77 | 84 |
| Alternate drawing sequence | 84.6 | 90 |

Tab. 5. Setting of boreholes
 Tab. 5. Parametry otworów wiertniczych do monitorowania przemieszczeń

| Device number | Dip in strike direction /° | Dip in vertical direction/° | Length of measurement device /m | Note |
|---------------|----------------------------|-----------------------------|---------------------------------|------------------------------|
| 1 | 45 | 8 | 21.5 | Distance to seam floor: 5.5m |
| 2 | 45 | 13 | 21.8 | Distance to seam floor: 7.5m |
| 3 | 45 | 25 | 23.3 | Distance to seam floor 12m |

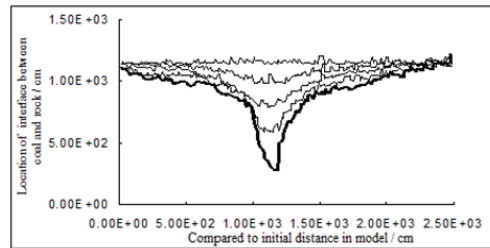


Fig. 12. Profile of interface between coal and rock during caving
 Rys. 12. Granicy między węglem a skałą stropową podczas zawałowania

vious any caving cycle. The distribution of top coal loss and top coal recovery under different caving spans are illustrated in Figure 8 and Table 3.

The calculation result shows that under the same cutting-caving height ratio of 1:2, the recovery rates in 0.8 m caving span were relatively high compared to those in a 1.6 m caving span. In particular, the absolute rate increased by 3.22%, and the relative rate increased by 5.06%. It is also observed from the model that the proportion of waste rock in recovered coal for a case of 0.8 m caving span was significantly larger than that for the case of 1.6 m caving span. It is concluded that 0.8 m caving span is the optimal design for face 3107.

4.3 Optimization of caving sequence

Figures 9, 10 and 11 display the distribution of interface between coal and waste rock in successive and alternate drawing sequences. The top coal recovery rate is given in Table 4.

According to the drawing principle mentioned above, the successive drawing sequence resulted in unevenly recovered top coal volumes. The interface between coal and rock was clearly skew, and waste rock significantly increased. In case of alternate drawing sequence, the interface was symmetrically distributed; the top coal was uniformly recovered, and the coal loss was remarkably reduced.

The numerical outputs in Table 1-6 demonstrate that the top coal recovery and seam recovery rates in the alternate sequence were 7.6% and 6%, respectively, which were larger than that those in successive sequence. In the alternate sequence, operation tasks were not mutually impacted. The drawing can be implemented in parallel at different doors that increases face production. The efficiency in equipment usage was optimal, and the operational tasks were simplified. To conclude, the alternate drawing sequence is the most optimal design for face 3107 Liang Baoshi coal mine.

4.4 Coal loss at gate ends

For a general LTCC face with a length in dip direction in a range of 120–150 m, coal seam loss is about 15%, top coal loss is 10%, coal loss at gate ends occupies 2%, and coal loss in installation and recovery roadways are about 3%. Since the length of face 3107 is only 81 m, coal loss at gate ends should be accordingly increased.

Empirical experience shows that for an ideal caving scenario, there should be no large caving block obstructing drawing door. Also, the roof strata at two gate end significantly sag downward. This makes the top coal above gate-end supports to move toward face supports, meaning that a large proportion of top coal at two face ends are recoverable.

It is observed from practice that final drawing angle of caved coal ranges from 40 to 43 degrees. Hence, the curve of the interface between coal and caved rock is used to determine coal loss at two ends. Figure 12 outlines the profile of the interface during caving.

From the PFC2D 2.10 model's output, a regression method was used to develop an equation for the interface before caving process. The equation is shown below:

$$Y = 0.0857 X^2 - 0.3234 X - 1.3415 \quad (1)$$

It is seen that the relationship between coal and waste rock was in a parabolic shape. The coal loss at the gate ends was finally calculated of 3.2%, for a top coal caving thickness of 5 m.

5. Field investigation of movement laws of top coal and immediate roof rock

To investigate the movement laws of the top coal and immediate roof rock, long boreholes were drilled in advance of the face and from tailgate roadway. The displacement was measured through extensometers placed inside the holes.

Tab. 6. Monitoring result of coal and rock movement at Face 3107

Tab. 6. Dane monitorowania przemieszczeń węgla i skał na przpodku 3107

| L (distance to face line/m) | 9 | 8 | 4 | 2 | 0 | -2 | -3.3 | -4 | -6 |
|-----------------------------|---|---|----|----|----|----|------|-----|-----|
| h=5.5m top coal | 6 | 9 | 19 | 42 | 69 | 97 | 156 | 226 | 581 |
| h=7.5m top coal | 5 | 8 | 17 | 36 | 63 | 89 | 147 | 214 | 531 |
| h=12m immediate roof | | 0 | 2 | 9 | 20 | 42 | 76 | 119 | 219 |

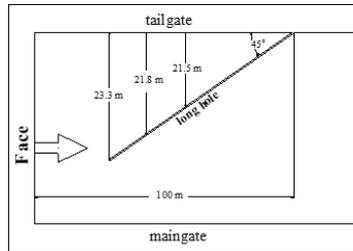


Fig. 13. Layout of observation long boreholes in tailgate roadway

Rys. 13. Rozmieszczenie otworów obserwacyjnych dla monitorowania przemieszczeń

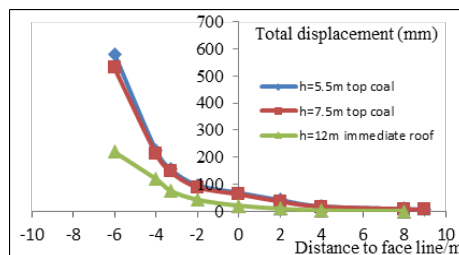


Fig. 14. Total displacement in coal and immediate rock of Face 3107 verse distance to face line

Rys. 14. Całkowite przemieszczenie na węglu i stropowej skale w odległości ściany 3107 względem linii ściany

5.1 Layout of boreholes

The holes were drilled 100 m ahead of face line and from tailgate roadway. An observation station was designed with four holes. In each hole, there were three displacement-measuring heads to monitor the deformation and movement of top coal and roof strata. Table 5 and Figure 13 display the setting and layout of long boreholes for observation.

The measurement method was as follows. In the same hole, three fixed measuring heads were connected via a steel wire. In the tailgate, the wire was connected to a displacement ruler. As the measuring head moved, the displacement was recorded daily.

5.2 Movement Laws of Top Coal and immediate Roof rock

Table 6 summarizes the data recorded for field measurement at Face 3107. Figures 14 show the total displacements of measuring heads compared to the face line.

The monitoring results show that as the face advanced, total displacements of top coal and immediate rock increased from some distances ahead of face line to the caving zone in geometric progression. Using a mathematical regression method, the laws of top coal and roof rock movement in different positions were developed:

$$h=5.5\text{m top coal} \quad S = 72.043 e^{-0.2832L} \text{ mm} \quad (2)$$

$$h=7.5\text{m top coal} \quad S = 65.197 e^{-0.2894L} \text{ mm} \quad (3)$$

$$h=12\text{m immediate rock} \quad S = 17.116 e^{-0.24562L} \text{ mm} \quad (4)$$

It can be seen from the equations that the movement laws at different locations followed a similar trend. For instance, at heights of 5.5 m and 7.5 m in top coal, the movement laws were almost identical. This proves that the breakage of top coal was ideal; that is, the failure was ubiquitous, and there was no caving in separate layers. Based on the displacement magnitude, the movement can be divided to be slow and fast, which are in the range of (10m, -3m) and (-3m, -6m), respectively.

It is also observed that the displacement magnitude of immediate rock was less than that of top coal. This means that there was a clear separation in movement between the immediate roof and top coal. The slow movements of roof rock above support and ahead of face line indicate a stable condition of the strata. For the immediate rock about 4 m behind the face line (towards caving zone), the displacement recorded was greater than 100 mm. This significant magnitude confirms the complete failure of the roof behind face support. The immediate roof caved as the face advanced and accordingly facilitated top coal caving. The caving angle was observed in range 65 to 70 degrees—a caving-favourable angle.

It can be concluded from the field measurement that the selected technological parameters of Face 3107 were optimal. They assisted top coal caving and increased top coal recovery rate in SLTCC.

6. Conclusion

Limited longwall face length in dip direction causes unfavourable caving condition for top coal and roof rock. The top coal caving zone height is limited. The upper portions of top coal and roof strata can form cantilever beams that cave in

delay and cause significant-top coal loss.

An increase in cutting height facilitates the failure and caving of top coal. However, when the height increases to a certain value, roof strata become less stable; face spall and top coal fall may occur that interrupt normal production.

For SLTCC technology, the design of the alternate drawing sequence is recommended because it increases the top coal recovery rate and face productivity. The operation tasks are simplified, and the use of equipment is optimized.

For geological condition of face 3107 of Liang Baoshi coal mine, the selection of 3 m cutting height, 0.8 m caving span,

and alternate drawing sequence maximizes top coal failure and recovery. The caving angle ranges from 65 to 70 degrees, and face recovery rate reaches up to 90%.

Acknowledgement

This research is funded by Hanoi University of Mining and Geology (HUMG) through Project T19-45. The State Key Laboratory of Coal Resources and Mine Safety of China University of Mining and Technology is thanked for providing field measurement data.

Literatura – References

1. BUI, M.T.; LIU, C.Y.; LE, T.D.; GUO, WEIBIN. Study on the stress distribution ahead of face when the ratio of cutting height to caving height varies in the extraction of extra-thick seam by Fully Mechanized Top Coal Caving technology. Proceedings of the 3rd international conference on advances in mining and tunneling 21-22 october (2014), VietNam, p.169-176.ISBN 978-604-913-248-3.
2. CAO, S.G.; MIAO, X.X. Ground pressure controlling on super-length fully-mechanized mining face with top-coal caving. Journal of China Coal Society (2001)26(6)621-625(In Chinese).
3. Itasca Consulting Group. "Universal Distinct Element Code (FLAC, PFC) Verification Problems and Example Applications," Minneapolis, Minnesota, USA, 2000.
4. LE, T.D.; OH, J.; HEBBLEWHITE, B.; ZHANG, C. & MITRA, R. A discontinuum modelling approach for investigation of Longwall Top Coal Caving mechanisms. International Journal of Rock Mechanics and Mining Sciences, 106 (2018) 84-95.
5. LIU, C.Y.; JIN, T. Dynamic bearing characters and reliability analysis of top coal caving hydraulic supports. Xu-zhou: Ground pressure and strata control (2005).
6. LIU, C.Y. Features of Support-surrounding Rock Inter-Action in Fully Mechanized Caving Face with High-Production and High-Efficiency. 13th International Conference on Coal Research 26-29 October, 2004 Shanghai China.
7. N.E, Yasitli B.; Unver. 3D numerical modeling of longwall mining with top-coal caving [J] International Journal of Rock Mechanics & Mining Sciences (2005/42/2) 219-235
8. XU, JIA.LIN.; JIN, M.G.; Study on coal and coal-bed methane simultaneous extraction technique on the basis of strata movement, journal of China Coal Society (2004), 29(2):129-132. (In Chinese). ZHANG, N.B.; LIU, C.Y.; PEI, M.S. Effects of caving-mining ratio on the coal and waste rocks gangue flows and the mount of cyclically caved coal in fully mechanized mining of super-thick coal seams. International journal of mining science and technology, Vol.25 No.1 (2015) 145-150.
9. https://books.google.com.vn/books?hl=vi&lr=&id=ywSiDwAAQBAJ&oi=fnd&pg=PA260&dq=Study+on+controlling+parameters+and+technological+optimization+of+Strip+Longwall+Top+Coal+Caving+in+thick+coal+seams&ots=S9ml5ax80Y&sig=_cQV2bTGNOgt9jpmiCnUHVzZQb8&redir_esc=y#v=onepage&q&f=false
10. <https://www.mdpi.com/2071-1050/10/3/700#cite>
11. http://en.cnki.com.cn/Article_en/CJFDTotal-KYYK201502002.htm
12. <https://onlinelibrary.wiley.com/doi/full/10.1002/ese3.660>.
13. <http://www.ejge.com/2014/Ppr2014.883ma.pdf>.

Badanie nad parametrami wpływu i optymalizacja technologii dla zmechanizowanego wyrobiska eksploatowanego zawałem przy grubych pokładach

W oparciu o warunki geologiczno-górnice przodka 3107 w kopalni Liang Baoshi w Chinach, oprogramowanie FLAC3D 2.10 i PFC2D 2.10 zostało wykorzystane do analizy parametrów wpływających na awarię, zawał i stopień odzysku węgla stropowego w zmechanizowanym wyrobisku eksploatacyjnym. Analizowanymi parametrami są długość przodka, wysokość urabiania, rozpiętość i kolejność zawału stropowego.

Wyniki pokazują, że zastosowanie SLTCC przy ograniczonej długości ściany nie sprzyja awariom węgla i zwiększa ubytki górne. Dlatego odpowiedni dobór parametrów technologicznych jest ważny dla efektywnej eksploatacji w grubych pokładach węgla. Wyniki liczbowe pokazują, że projekt przodka o 3 m wysokości urabiania, 0,8 m rozpiętości zawału i z naprzemienną kolejnością skutkuje wysoką wydajnością wydobywania węgla, prostą technologią wydobywczą i wydajną pracą urządzeń przodkowych.

Słowa kluczowe: obudowe zmechanizowane, technologia zawałowania, współczynnik odzysku węgla, grube pokłady